RSC Advances

PAPER

View Article Online
View Journal | View Issue

Cite this: *RSC Adv.*, 2019, **9**, 30943

A novel ratiometric fluorescent probe for the selective determination of HClO based on the ESIPT mechanism and its application in real samples†

Jingrui Li,[ab] Aijun Gong,[*ab] Guoqing Shi[a] and Chengwen Chai[a]

Received 18th June 2019
Accepted 15th September 2019

DOI: 10.1039/c9ra04569d

rsc.li/rsc-advances

Based on the ESIPT fluorescence mechanism, herein, a novel ratiometric fluorescent probe was designed and synthesized for the detection of HClO. The reaction site of diaminomaleonitrile at the *ortho*-position of the phenolic hydroxyl group made the probe exhibit a ratiometric fluorescence response towards hypochlorous acid (HClO). The specific sensing mechanism was verified *via* MS, HPLC and ^{1}H NMR spectroscopy. Moreover, the probe showed excellent performance with high sensitivity and good selectivity towards HClO in the presence of other reactive oxygen species. In addition, the probe was successfully applied to detect HClO spiked in tap water, river water and diluted human serum with good recoveries.

1. Introduction

In our modern daily life, for clean drinking water, hypochlorous acid (HClO) is widely used as a common disinfectant, especially in water treatment and distribution; in addition, HClO is used on a large scale in the food industry. As one of the natural oxidants, HClO can be dissociated into hypochlorite anion (OCl^-) under physiological conditions ($pK_a = 7.46$).[1] In biology, its oxidation property make it react with many biomolecules such as DNA, RNA, fatty acid groups, cholesterol and proteins. HClO as a typical reactive oxygen species (ROS) plays an important role in some pathological and biological events;[2] for instance, HClO mediates the peroxidation of chloride ions in activated leukocytes[3] and acts as a critical microbicidal agent in response to inflammatory stimuli; moreover, the abnormal generation of HClO from phagocytes can cause many inflammation-related diseases including cardiovascular and cancer,[4] neurodegeneration,[5] renal disease[6] and osteoarthritis.[7]

Compared to traditional analytical techniques, such as electroanalysis, chemiluminescence, or chromatography, used for the determination of HClO, fluorescence detection[8–10] has been found to be superior in some aspects such selectivity and sensitivity. The fluorescence method also meets the requirement of a fast response and real-time detection, which is appropriate for the investigation of HClO in complicated and living systems.[11–14] Therefore, many fluorescent probes have been designed and developed in recent years. Wang *et al.*[15] developed an effective method for the imaging of lysosomal HClO to better understand its role in HClO-related diseases. Xue *et al.*[16] designed a simple and efficient ratiometric fluorescent nanoprobe for the imaging of exogenous/endogenous HClO in lysosomes. Zhang *et al.*[17] developed a lysosome-targetable fluorescent probe for HClO detection by combining a 4-(2-aminoethyl)-morpholine moiety and a HClO-capturing group phenyl-thiourea together. Yang *et al.*[18] synthesized a fluorescent probe for the quantitative detection of HClO and live cell imaging, which provided a powerful tool for the investigation of HClO. Peng *et al.*[19] reported a BODIPY-based HClO probe with high sensitivity and fast response that was applied to image basal HClO in cancer cells. In addition to the abovementioned fluorophores, the other fluorophores used in probe designs include coumarin,[20] rhodamine,[21] heptamine cyanine[22] and iridium complexes.[23]

2-(2′-Hydroxyphenyl)benzimidazole (HBI) is a typical fluorescent compound, which emits intense fluorescence *via* an excited-state intramolecular proton transfer (ESIPT) reaction. Its unique characteristic of a large Stokes shift (>100 nm) with a good quantum yield (40–65%, in aqueous solution) makes it suitable for wide applications in laser dyes, high-energy radiation detectors and fluorescence imaging. Most of the probes synthesized on the basis of HBI or its derivatives exhibit fluorescence emission of a typical "turn-on" type. He *et al.*[24] reported a highly selective and sensitive probe for HClO detection by choosing HBI as a fluorophore. Compared to "turn-on" probes, the ratiometric fluorescent probes are more reliable because these probes can reduce the detection error by self-calibration based on two fluorescence emission bands; however, to date, only few ratiometric fluorescent probes have been designed based on HBI or specifically used for HClO detection.

[a]*School of Chemistry and Biological Engineering, University of Science and Technology Beijing, Beijing 100083, China. E-mail: Gongaijun5661@ustb.edu.cn; Fax: +86-010-62334071; Tel: +86-010-82375661*

[b]*Beijing Key Laboratory for Science and Application of Functional Molecular and Crystalline Materials, University of Science and Technology Beijing, Beijing 100083, China*

† Electronic supplementary information (ESI) available. See DOI: 10.1039/c9ra04569d

Therefore, in this study also, HBI was chosen as a fluorophore for the synthesis of a novel ratiometric probe. Diaminomaleonitrile was taken as the reaction site for the sensor design. Compared to the former ESIPT fluorophore HBO (2-(2′-hydroxyphenyl)-benzoxazole),[25] the fluorescent response group diaminomaleonitrile led to a ratiometric probe that was fluorescence emission type instead of intensity-based type. Upon the addition of HClO, the probe subsequently reacted with it to realize hypochlorous acid-initiated oxidative intramolecular cyclization, thus providing a rapid and sensitive fluorescence response towards HClO. Due to its improved performance, the probe could be applied to detect HClO in tap water, river water and diluted human serum samples.

2. Experimental

2.1 Reagents and instruments

All the solvents and reagents employed herein were obtained from commercial suppliers and used directly without any further purification. Herein, the UV-vis spectra were obtained using the UV-vis spectrophotometer UV-8000S (Shanghai Metash Instruments Co., Ltd.). The fluorescence spectra in this study were obtained using the fluorescence spectrophotometer FS5 (Edinburgh Instruments). Quantum yield measurements were carried out using a spectrofluorometer (FS5) equipped with an integrating sphere. The ^{1}H NMR and ^{13}C NMR spectra were obtained using the Bruker AV-300 spectrometer (Bruker), with chemical shifts reported as ppm (in $CDCl_3$ and DMSO-d_6, with TMS as the internal standard). Mass spectra analysis was carried out using the LCQ Fleet mass spectrometer (Thermo Fisher).

2.2 Synthesis of the probe

In a round-bottom flask equipped with a magnetic stirring bar, 5-methylsalicyladehyde (136 mg, 1 mmol) and sodium bisulfite (104 mg, 1 mmol) were dissolved in ethanol (15 mL). The solution was stirred at room temperature for 4 h. Then, the solution of *o*-diaminobenzene (108 mg, 1 mmol) dissolved in ethanol (5 mL) was added to the flask and heated to reflux for 4 h. The reaction was quenched by pouring the solution into ice water. After a few minutes, a white solid precipitated from the aqueous phase. The crude product, *i.e.* compound **1**, was obtained by filtration under diminished pressure, and then, it was applied directly in the next step for the synthesis of the fluorescent probe without any purification (168 mg, 75% yield). ^{1}H NMR (300 MHz, DMSO-d_6) δ 13.13 (s, 1H), 12.86 (s, 1H), 7.90–7.83 (m, 1H), 7.69 (d, J = 7.5 Hz, 1H), 7.58 (d, J = 7.5 Hz, 1H), 7.27 (p, J = 5.4 Hz, 2H), 7.18 (ddd, J = 8.4, 2.2, 0.7 Hz, 1H), 6.92 (d, J = 8.3 Hz, 1H), 2.31 (s, 3H). MS (ESI): calcd for $C_{14}H_{12}N_2O$: 224.09; found: 225.39.

The compound **2** was synthesized according to the Duff reaction. Typically, compound **1** (112 mg, 0.5 mmol) and hexamethylenetetramine (HMTA, 210 mg, 1.5 mmol) were dissolved in trifluoroacetic acid (15 mL). The mixture was heated and refluxed for 8 h under the protection of nitrogen gas. The reaction was quenched by pouring the solution into ice water. The obtained solution was adjusted to neutral with sodium hydroxide. A yellow solid precipitated from the solution. The product was obtained through filtration and purified with silica chromatography using hexane–ethyl acetate (10 : 1) as the eluent to obtain a pure product (70 mg, 56% yield). ^{1}H NMR (300 MHz, DMSO-d_6) δ 13.84 (s, 3H), 10.47 (s, 1H), 8.19 (dd, J = 2.2, 0.8 Hz, 1H), 7.68 (dt, J = 8.0, 4.0 Hz, 2H), 7.60 (dd, J = 2.2, 0.9 Hz, 1H), 7.37–7.25 (m, 2H), 2.36 (t, J = 0.7 Hz, 3H). MS (ESI): calcd for $C_{15}H_{12}N_2O_2$: 252.09; found: 253.62.

Compound **2** was reacted with diaminomaleonitrile to obtain the probe. Compound **2** (51 mg, 0.2 mmol) and diaminomaleonitrile (22 mg, 0.2 mmol) were dissolved in EtOH (15 mL). Then, 3 drops of acetic acid were added to the mixture. The solution was further refluxed for 5 hours under N_2 gas protection. The final yellow solution was concentrated to obtain precipitates, which were filtered off and washed with EtOH. The product was recrystallized in EtOH to obtain a yellow solid (41 mg, 60% yield). ^{1}H NMR (300 MHz, DMSO-d_6, TMS): δ 13.37 (s, 1H), 8.71 (s, 1H), 8.20 (d, J = 2.1 Hz, 1H), 8.02 (d, J = 2.2 Hz, 1H), 7.95 (s, 2H), 7.67 (s, 1H), 7.30 (d, J = 7.4 Hz, 1H), 2.37 (s, 3H). MS (ESI): calcd for $C_{19}H_{14}N_6O$: 342.12; found: 343.36.

2.3 Fluorescence detection procedure

The stock solution of the probe was prepared by dissolving the probe in methanol. All the stock solutions of the other analytes were obtained by dissolving them in ultra-pure water (see ESI†). The fluorescence properties of the probe were investigated in PBS/MeOH (v/v, 4 : 1, pH = 7.4, 10 mM). Each spectrum was obtained after 1 min. The detection limit (LOD) was calculated based on the fluorescence titration reported in the literature. The fluorescence intensity of ten blank samples was measured. Then, the corresponding mean value and the standard deviation were calculated. Moreover, LOD was calculated based on the formula LOD = $3\sigma/k$, where σ is the standard deviation of the blank samples measured 11 times and k is the slope obtained from the calibration curve.

The quantum yields (QY,η) of the probe and the probe–HClO system were determined according to the literature.[25,26] All the data were acquired in PBS/MeOH (v/v, 4 : 1, pH = 7.4, 10 mM). The QY, defined as the ratio of the emitted photons to the absorbed photons, was determined according to the following expression:

$$\eta = \frac{\text{number of photons emitted}}{\text{number of photons absorbed}} = \frac{L_{\text{sample}}}{E_{\text{reference}} - E_{\text{sample}}}$$

where η represents QY, L_{sample} is the emission intensity, and $E_{\text{reference}}$ and E_{sample} are the intensities of the excitation light not absorbed by the reference and the sample, respectively.

3. Results and discussion

3.1 Probe design and synthesis

In the probe proposed herein, HBI was used as a fluorophore, which generated fluorescence under ultraviolet excitation; its unique ESIPT process endowed the probe with excellent fluorescence properties such as a large Stokes shift (>100 nm) and fast fluorescence response towards HClO. As a typical

fluorophore based on the ESIPT mechanism, HBI emits intense fluorescence *via* an excited-state intramolecular proton-transfer reaction, which guarantees fluorescence emission during the detection process. On the other hand, the reaction site on the probe could change the fluorescence emission type to realize the detection of HClO.

In this study, HBI-CH_3 was easily obtained under mild conditions. Without any purification, it could be directly used in the following reaction. The introduction of an aldehyde group was realized through the reaction of HBI-CH_3 with hexamethylenetetramine (HMTA) in an acid solution; the final reaction to synthesize the probe involved the stirring of HBI-CHO and diaminomaleonitrile in methanol under reflux conditions. The introduction of a reaction site at the *ortho*-position of the phenolic hydroxyl group caused the corresponding probe to exhibit different fluorescence emissions. Its fluorescence property and detection mechanism were investigated *via* the following experiments (Scheme 1).

3.2 Fluorescence response of the probe toward HClO

The fluorescence property of the probe was investigated in PBS/MeOH (v/v, 4 : 1, pH = 7.4, and 10 mM) at room temperature. As shown in Fig. 1, the probe displayed a fluorescence emission band at 600 nm. Upon the addition of HClO, a new fluorescence emission band appeared at 485 nm. Its fluorescence intensity at 485 nm gradually increased with an increase in the amount of HClO. However, the fluorescence intensity at 600 nm did not change and maintained its original level. Therefore, the probe exhibited a ratiometric characteristic towards HClO. By plotting the fluorescence intensity ratio (FI_{485}/FI_{600}) *versus* the concentration of HClO, a good linear relationship was obtained in the concentration range from 2.0 μM to 45.0 μM. The detection limit was calculated to be 14.6 nM based on $3\sigma/k$. The result proved that the probe could quantitatively and qualitatively determine HClO with a low detection limit. Based on the abovementioned experimental results, it can be concluded that the proposed probe shows some advantages over the other probes listed in Table 1 in terms of the detection solvents, Stokes shift, detection limit and response time; this indicates

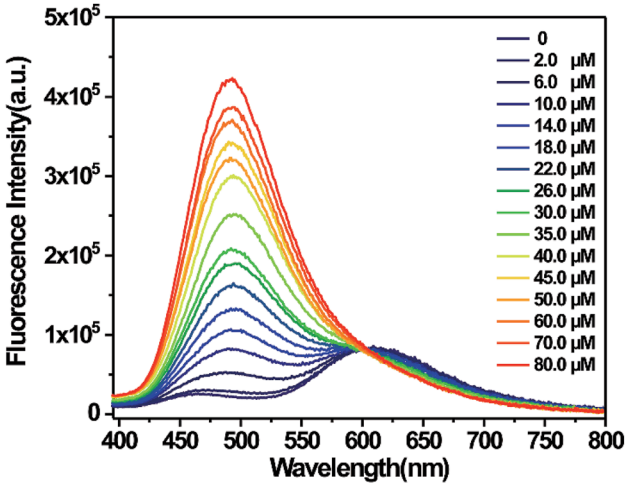

Fig. 1 Fluorescence spectral changes of the probe (10 μM) in PBS/MeOH (v/v, 4 : 1, pH = 7.4, and 10 mM) upon the addition of different amounts of HClO (2.0–80.0 μM). Fluorescence intensity was determined 1 min after the addition of HClO at room temperature (slit width: 2/8 nm, λ_{ex} = 340 nm).

that the probe proposed herein has great potential in HClO detection (Fig. 2).

Moreover, the UV-vis absorption of the probe was investigated. As shown in Fig. 3, the probe exhibited an absorption band between 350 nm and 425 nm with a peak centered at 400 nm. Upon the addition of HClO, the absorption band at 400 nm went down to the lower absorption value. However, a new absorption band at 335 nm appeared in the spectrum. HClO was added to the detection solution to react with the probe, leading to the fluorescence and UV-vis response. The specific detection mechanism was investigated to explain the internal changing processes.

From the initial investigation of the fluorescence properties, it was clear that the introduction of diaminomaleonitrile did not quench the fluorescence. Thus, the proposed probe is fluorescence intensity ratio type.

3.3 Time-dependent fluorescence response

In addition, the time-course fluorescence response of the probe towards HClO was tested. As shown in Fig. 4, upon the addition of 26 and 60 μM HClO, the fluorescence ratio (FI_{485}/FI_{600}) increased significantly and reached a maximum value within 30 seconds. This result showed that the probe exhibited a kind of 'fast response' characteristic for HClO and could be appropriate for the real-time detection of HClO.

3.4 Selectivity of the probe

The selectivity of the probe towards HClO was also investigated. The interfering components could be divided into three categories: anions, metal cations and ROS. Other reactive oxygen species (ROS) were chosen to verify the probe's fluorescence response towards them. The preparation details of ROS, which include $^1O_2$, $^{\bullet}OH$, H_2O_2, Fe^{3+}, $ONOO^-$, NO, and ^{t}BuOOH, are provided in the ESI.†

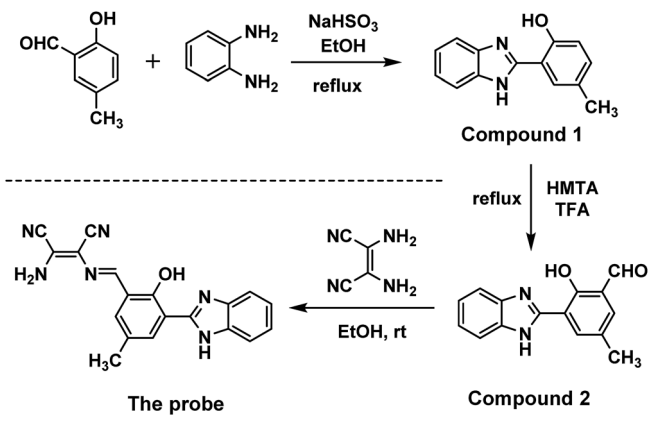

Scheme 1 Synthesis of the probe.

Table 1 Typical ratiometric fluorescent probes for the determination of HClO

Probe	λ_{ex} (nm), λ_{em} (nm)	Detection solvent	Detection limit	Response time	Ref.
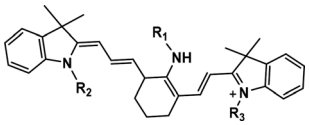	530, 605/760	PBS	100 nM	10 min	27
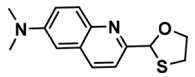	360, 492/562	PBS, pH7.4, 5% DMF	89 nM	1 min	28
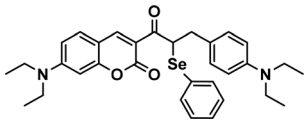	475, 495/618	PBS, pH7.4, 1% ACN	4.6 nM	200 s	29
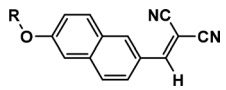	350, 425/600	PBS, pH7.4, 10% DMSO	15.2 nM	50 s	30
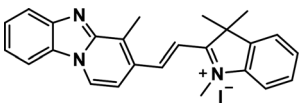	475, 512/653	PBS, pH6.0, 50% ACN	56 nM	13 min	31
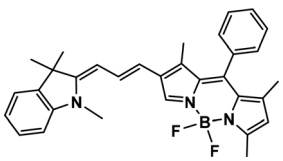	488, 511/713	PBS, pH7.4, 50% EtOH	10.6 nM	10 s	32
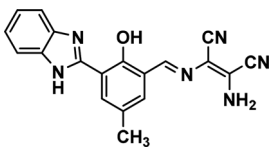	340, 485/600	PBS/MeOH (v/v, 4 : 1)	14.6 nM	30 s	This work

As shown in Fig. 5, the commonly used anions did not affect the detection. All the chosen metal cations did not produce new interference, except for the copper ions. The copper ions could quench the fluorescence of HBI.[33] Most importantly, other ROS also did not trigger an increase in the fluorescence of the probe. Especially, the probe exhibited about an 8-fold increase in the

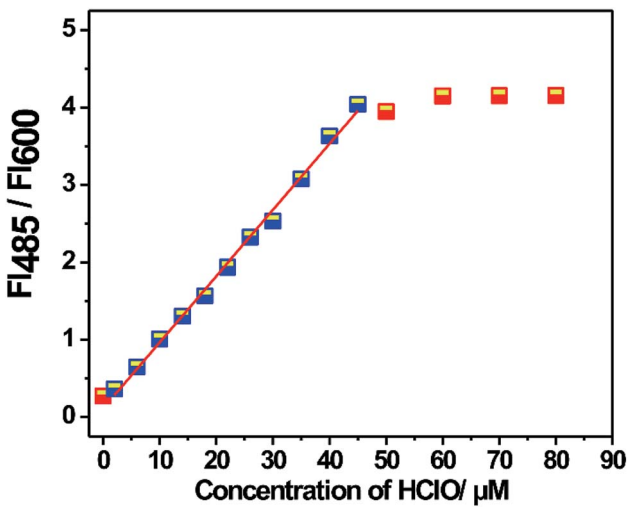

Fig. 2 A linear relationship between the fluorescence ratio for the probe (10 μM) and the HClO concentration (2.0–45.0 μM). Fluorescence intensity was determined 1 min after the addition of HClO at room temperature (slit width: 2/8 nm, λ_{ex} = 340 nm).

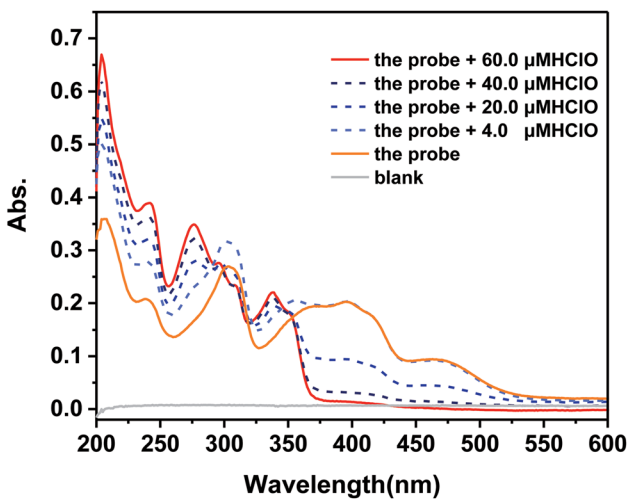

Fig. 3 UV-vis absorption spectra of the probe in PBS/MeOH (v/v, 4 : 1, pH = 7.4, and 10 mM) upon the addition of different amounts of HClO (4.0, 20.0, 40.0, and 60.0 μM).

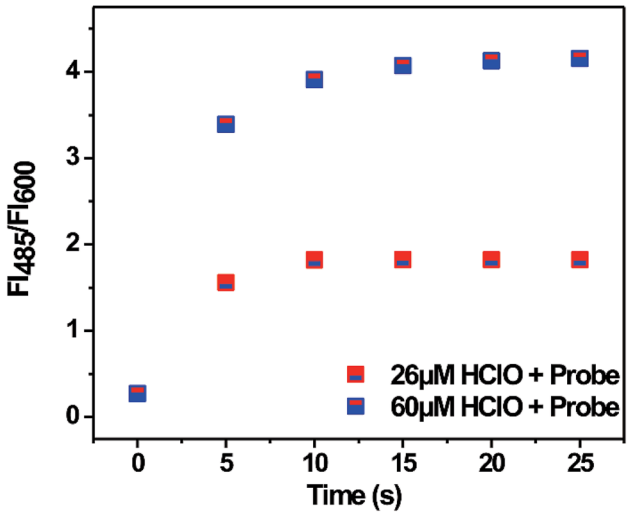

Fig. 4 Time-dependent fluorescence ratio (FI_{485}/FI_{600}) of the probe (10 μM) towards HClO (26 μM and 60 μM) in PBS/MeOH (v/v, 4 : 1, pH = 7.4, and 10 mM). Fluorescence intensity was determined 1 min after the addition of HClO at room temperature (slit width: 2/8 nm, λ_{ex} = 340 nm).

fluorescence intensity ratio towards HClO over other ROS. The competition experiment results were in agreement with the abovementioned results. These results demonstrate the selectivity of the probe for HClO.

3.5 Effect of pH on the fluorescence emission of the probe

The influence of pH on the detection assay was also investigated. In real sample detection, pH is important for the application of a probe. Therefore, the effect of pH on the emission spectra of the probe was investigated. As shown in Fig. 6, pH did not exert an obvious influence on the fluorescence intensity of the probe at 600 nm over the range from pH 4.0 to 9.0. Upon the addition of HClO, the fluorescence intensity of the probe at 600 nm did not change, and a new fluorescence emission at 485 nm appeared but did not show a significant difference. When the added concentration of HClO was 60 μM, the fluorescence intensity ratio (FI_{485}/FI_{600}) was maintained at 4.2 from pH 4.0 to 9.0. This result indicated that the probe could potentially be applied for determining HClO in real samples.

3.6 Detection mechanism

According to the literature,[34,35] there are two kinds of typical detection mechanisms (Scheme 2): hypochlorous acid-initiated oxidative intramolecular cyclization and removal of the unbridged imine C=N bond. The designed probes based on the abovementioned two chemical reactions were fluorescent "turn-on" types. Although the recognition functional group was the same as that in the former probes, the fluorescence emission type of the probe in this study was different. Therefore, it was urgent to investigate the mechanism involved in the fluorescence detection.

To verify the detection mechanism of the probe for HClO in a detection solution, related experiments were performed. At first, the detection solution was directly injected into the mass spectrometer to mainly analyze its composition. Based on the obtained MS spectrum (Fig. 7), it was preliminarily concluded that the probe reacted with HClO in solution and converted to a new species, which was assigned to the new peak at *m*/*z* 339.18. Moreover, when the probe reacted with a 3 equivalent amount of HClO, the probe was completely converted to a new species (inner table in Fig. 7). This reaction was not affected by the pH of the detection solution, which was in agreement with the effect of pH on the fluorescence emission of the probe. The new species at *m*/*z* 339.18 was the unique product of the detection reaction.

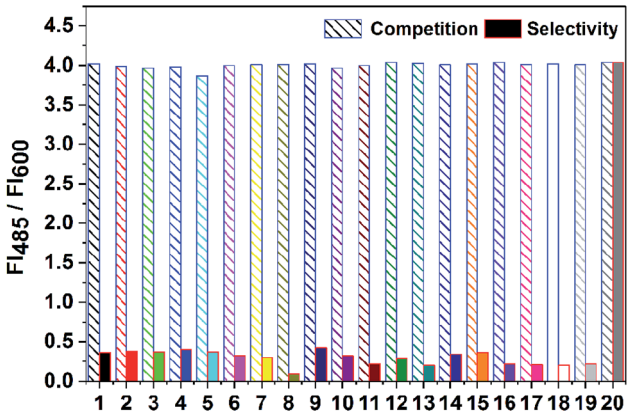

Fig. 5 Fluorescence response of the probe (10 μM) toward anions (50 μM), metal cations (50 μM), and ROS in PBS/MeOH (v/v, 4 : 1, pH = 7.4, 10 mM). (1) $^1O_2$, (2) $^{\bullet}OH$, (3) H_2O_2, (4) Fe^{3+}, (5) $ONOO^-$, (6) NO, (7) ^tBuOOH, (8) Cu^{2+}, (9) Zn^{2+}, (10) Ca^{2+}, (11) Cd^{2+}, (12) Fe^{2+}, (13) Co^{2+}, (14) Al^{3+}, (15) CH_3COO^-, (16) Hg^{2+}, (17) Mg^{2+}, (18) Na^+, (19) K^+, and (20) HClO. Fluorescence intensity was determined 1 min after the addition of HClO at room temperature (slit width: 2/8 nm, λ_{ex} = 340 nm).

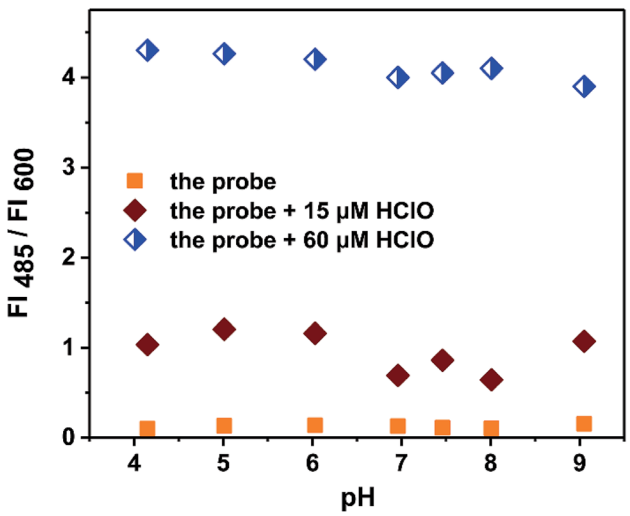

Fig. 6 Effect of pH on the fluorescence ratio (FI_{485}/FI_{600}) of the probe (15 μM) in the absence/presence of HClO (15 μM and 60 μM). Fluorescence intensity was determined 1 min after the addition of HClO at room temperature (slit width: 2/8 nm, λ_{ex} = 340 nm).

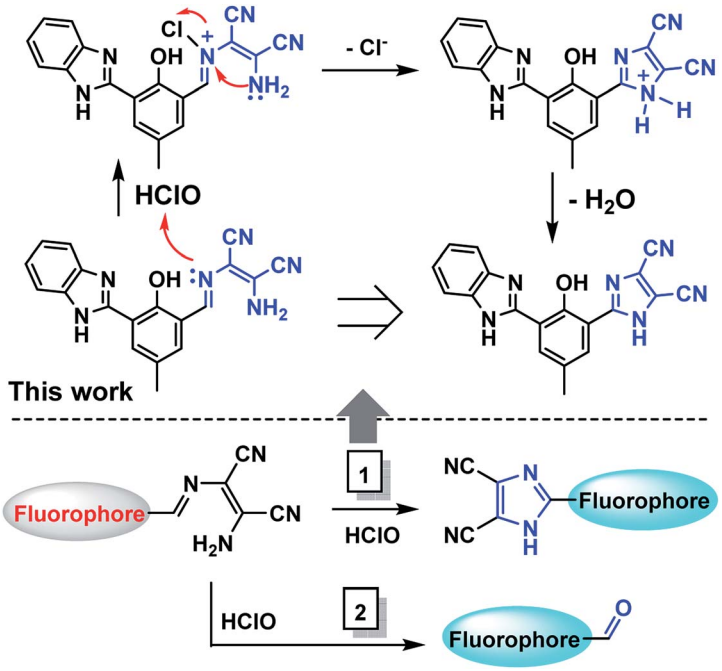

Scheme 2 Detection mechanism of the probe towards HClO.

Subsequently, we tried to separate the product generated in the detection reaction through HPLC. The concentration of the probe in the detection solution was increased to meet the test requirement. After optimizing the instrumental conditions, the components of the detection solution were efficiently separated. As shown in Fig. S3,† compared to the chromatogram of the probe with the detection solution, a new peak at the retention time of 7.25 min appeared, which could be attributed to the new species. The mobile phase effluent at this retention time was obtained, concentrated and directly injected into the mass

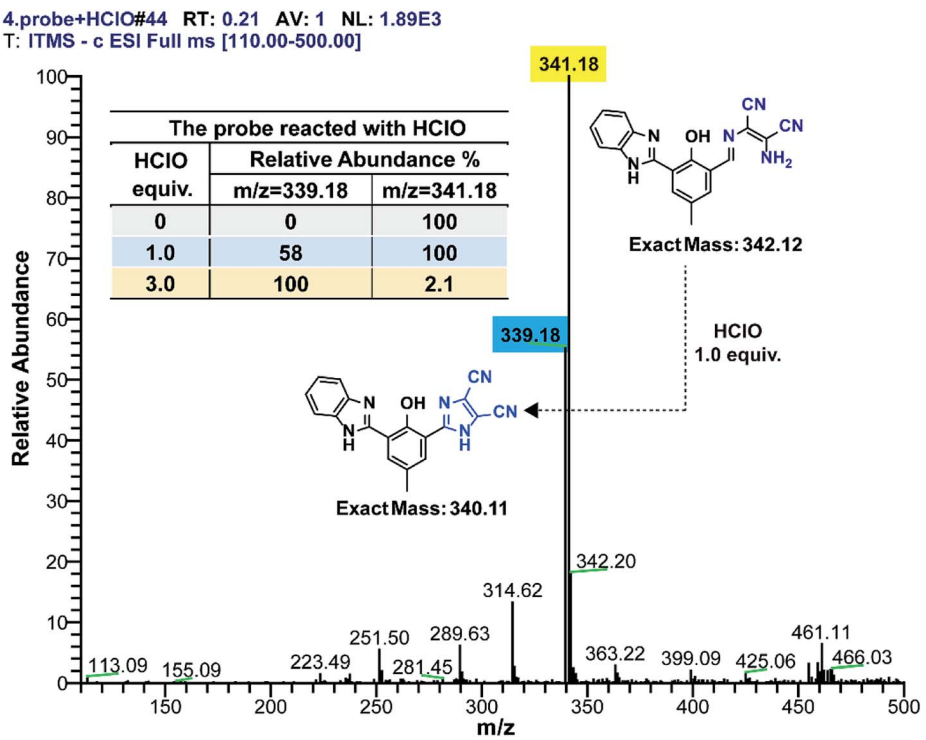

Fig. 7 Mass spectrum of the probe (10 μM) treated with HClO (inner table: 0, 10, and 30 μM).

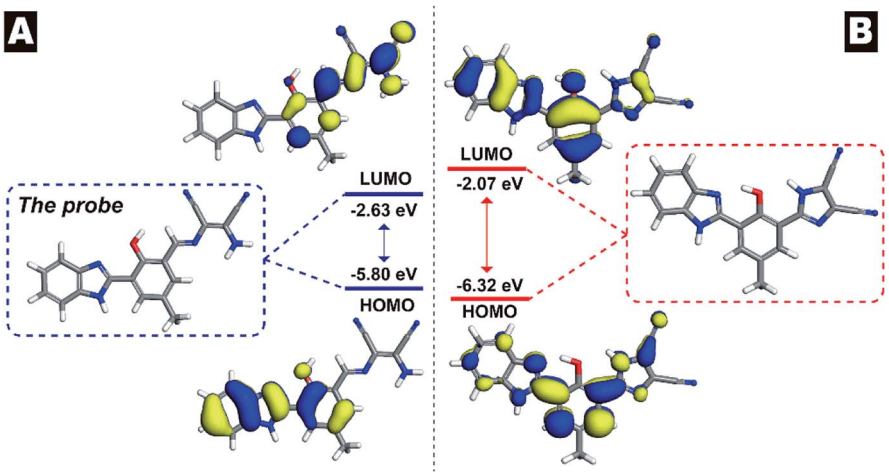

Fig. 8 Molecular orbital surfaces and energy levels obtained using the DFT/B3LYP method for the probe and its corresponding product.

spectrometer to confirm its exact molecular weight. The result showed that the molecular ion peak was at *m/z* 339.18, which was identical to the new peak shown in Fig. 7. It was concluded that the detection mechanism was as follows: the probe reacted with HClO in the detection solution and was converted to an intramolecular cyclization product. This proposed sensing mechanism is in agreement with the mechanism reported in the literature (Scheme 2, path 2).

Finally, the fluorescent product in the detection solution was isolated and characterized by ^{1}H NMR to clarify the actual reaction between the probe and HClO. As shown in Fig. S6,† a signal of the Schiff base proton at δ 8.73 ppm appeared in the spectrum of the probe but disappeared in the product; this indicated that the substituted imidazole structure was generated in the product.[34]

3.7 Theoretical computation of the probe

To better understand the geometry and electron density of the probe and its product, the Material Studio software was used to conduct a basic computational investigation; density functional theory (DFT) calculations with the Becke-3-Lee-Yang-Parr (B3LYP) exchange functional were performed using the DMol^3 package of the software.

Via the analysis of the product generated in the detection solution, the molecular orbitals of the probe and its product were obtained (Fig. 8). In Fig. 8, the highest occupied molecular orbital (HOMO) and the lowest unoccupied molecular orbital (LUMO) plots of the probe and its product are plotted. The 3D isosurface HOMO of the probe was mainly located on the fluorophore. The electronic spatial distributions indicated that the ESIPT process of the probe was not broken, which guaranteed fluorescence emission of the probe; on the other hand, the LUMO of the probe showed that the reaction with HClO most probably occurred on the C=N bond. When the HClO-initiated oxidative intramolecular cyclizing reaction was completed, the energy difference of the product was much larger than that of the probe, suggesting that the product was more chemically stable than the probe.

Table 2 Determination of HClO in real samples

Sample	Spiked/μM	Found/μM	Recovery/%	RSD/%
Tap water	0	2.0	—	—
	3.0	5.1	104.0	1.5
River water	5.0	4.9	98.8	2.1
	10.0	10.2	102.0	1.4
Human serum	5.0	4.9	98.0	3.0
	10.0	9.2	92.1	1.6

3.8 Detection of HClO in real samples

Briefly, tap water was obtained from our laboratory and directly used for detection without any pretreatment. The river water was obtained from the Xiaoqing River near Beijing North Fifth Ring Road. Before detecting HClO, the river water was filtered to remove the solid impurities. Finally, pretreatment for human serum was conducted as follows: 1.0 mL acetonitrile was added to 5.0 mL human serum and mixed thoroughly to precipitate the proteins. Then, the mixture was centrifuged to obtain the supernatant. The supernatant was diluted 50 times with PBS buffer (containing 20% ethanol, v/v, and pH 7.0). These real samples were spiked with the NaClO stock solution at the concentration of 100 μmol L^{-1} and investigated by the above-mentioned established analytical method.

The detection results are summarized in Table 2. When the real samples were spiked with the HClO solution of known concentration, the total concentrations in the samples were determined through the established method. Good recoveries from 92.1% to 104.0% with the RSDs from 1.4% to 3.0% were obtained. The abovementioned results indicated that the probe could quantify HClO in real samples.

4. Conclusion

In summary, a novel ratiometric fluorescent probe for the fast determination of HClO was designed and synthesized based on

the ESIPT fluorophore HBI. The probe exhibited high selectivity for the detection of HClO over a wide pH range. Through MS and HPLC, the specific sensing mechanism was determined. Finally, the probe was applied to determine HClO spiked in real samples, and the results indicated high potential of the probe in analytical and bioanalytical applications.

Conflicts of interest

The authors declare no competing financial interest.

Acknowledgements

This work was financially supported by National Key R&D Program of China (2018YFF0212503) and National Key R&D Program of China No. 2017YFF0106006. We thank Dr Wang from school of chemistry and biological engineering for providing the theoretical computation of the probe and its product.

References

1 D. C. Harris, *Exploring Chemical Analysis*, 4th edn, 2009, p. 538.
2 M. K. Shigenaga, T. M. Hagen and B. N. Ames, Oxidative damage and mitochondrial decay in aging, *Proc. Natl. Acad. Sci. U. S. A.*, 1994, **91**, 10771–10778.
3 X. Q. Chen, X. Z. Tian, I. Shin and J. Yoon, Fluorescent and luminescent probes for detection of reactive oxygen and nitrogen species, *Chem. Soc. Rev.*, 2011, **40**, 4783–4804.
4 D. I. Pattison and M. J. Davies, Evidence for rapid inter- and intramolecular chlorine transfer reactions of histamine and carnosine chloramines: implications for the prevention of hypochlorous-acid-mediated damage, *Biochemistry*, 2006, **45**, 8152–8162.
5 Y. W. Yap, M. Whiteman and N. S. Cheung, Chlorinative stress: An underappreciated mediator of neurodegeneration signaling?, *Cell*, 2007, **19**, 219–228.
6 S. M. Wu and S. V. Pizzo, α2-Macroglobulin from rheumatoid arthritis synovial fluid: functional analysis defines a role for oxidation in inflammation, *Arch. Biochem. Biophys.*, 2001, **391**, 119–126.
7 M. J. Steinbeck, L. J. Nesti, P. F. Sharkey and J. Parvizi, Myeloperoxidase and chlorinated peptides in osteoarthritis: potential biomarkers of the disease, *J. Orthop. Res.*, 2007, **25**, 1128–1135.
8 J. T. Hou, M. Y. Wu, K. Li, J. Yang, K. K. Yu, Y. M. Xie and X. Q. Yu, Mitochondriatargeted colorimetric and fluorescent probes for hypochlorite and their applications for *in vivo* imaging, *Chem. Commun.*, 2014, **50**, 8640–8643.
9 F. Ma, M. T. Sun, K. Zhang, Y. J. Zhang, H. J. Zhu, L. J. Wu, D. J. Huang and S. H. Wang, An oxidative cleavage-based ratiometric fluorescent probe for hypochlorous acid detection and imaging, *RSC Adv.*, 2014, **4**, 59961–59964.
10 W. Lin, L. Long, B. Chen and W. Tan, A ratiometric fluorescent probe for hypochlorite based on a deoximation reaction, *Chem.–Eur. J.*, 2009, **15**, 2305–2309.
11 Y. R. Zhang, Z. M. Zhao, J.-Y. Miao and B.-X. Zhao, A ratiometric fluorescence probe based on a novel FRET platform for imaging endogenous HOCl in the living cells, *Sens. Actuators, B*, 2016, **229**, 408–413.
12 Y. R. Zhang, N. Meng, J. Y. Miao and B. X. Zhao, A ratiometric fluorescent probe based on a through-bond energy transfer system for imaging HClO in living cells, *Chem.–Eur. J.*, 2015, **21**, 19058–19063.
13 H. D. Xiao, J. H. Li, J. Zhao, G. Yin, Y. W. Quan, J. Wang and R. Y. Wang, A colorimetric and ratiometric fluorescent probe for ClO- targeting in mitochondria and its application in vivo, *J. Mater. Chem. B*, 2015, **3**, 1633–1638.
14 P. Zhang, H. Wang, Y. Hong, M. Yu, R. Zeng, Y. Long and J. Chen, Selective visualization of endogenous hypochlorous acid in zebrafish during lipopolysaccharide-induced acute liver injury using a polymer micelles-based ratiometric fluorescent probe, *Biosens. Bioelectron.*, 2018, **99**, 318–324.
15 H. Wang, P. Zhang, Y. Hong, B. Zhao, P. Yi and J. Chen, Ratiometric imaging of lysosomal hypochlorous acid enabled by FRET-based polymer dots, *Polym. Chem.*, 2017, **8**, 5795–5802.
16 M. Xue, H. Wang, J. Chen, J. Ren, S. Chen, H. Yang, R. Zeng, Y. Long and P. Zhan, Ratiometric fluorescent sensing of endogenous hypochlorous acid in lysosomes using AIE-based polymeric nanoprobe, *Sens. Actuators, B*, 2019, **282**, 1–8.
17 P. Zhang, H. Wang, D. Zhang, X. Zeng, R. Zeng, L. Xiao, H. Tao, Y. Long, P. Yi and J. Chen, Two-photon fluorescent probe for lysosome-targetable hypochlorous acid detection within living cells, *Sens. Actuators, B*, 2018, **255**, 2223–2231.
18 J. Hu, N. Wong, M. Lu, X. Chen, S. Ye, A. Zhao, P. Zhao, R. Kao, J. Shen and D. Yang, HKOCl-3: a fluorescent hypochlorous acid probe for live-cell and *in vivo* imaging and quantitative application in flow cytometry and a 96-well microplate assay, *Chem. Sci.*, 2016, **7**, 2094–2099.
19 H. Zhu, J. Fan, J. Wang, H. Mu and X. Peng, An "enhanced PET"-based fluorescent probe with ultrasensitivity for imaging basal and elesclomol-induced HClO in cancer cells, *J. Am. Chem. Soc.*, 2014, **136**, 12820–12823.
20 J. Zha, B. Fu, C. Qin, L. Zeng and X. Hu, A ratiometric fluorescent probe for rapid and sensitive visualization of hypochlorite in living cells, *RSC Adv.*, 2014, **4**, 43110–43113.
21 J. T. Hou, M. Y. Wu, K. Li, J. Yang, K. K. Yu, Y. M. Xie and X. Q. Yu, Mitochondria-targeted colorimetric and fluorescent probes for hypochlorite and their applications for *in vivo* imaging, *Chem. Commun.*, 2014, **50**, 8640–8643.
22 G. Cheng, J. Fan, W. Sun, J. Cao, C. Hu and X. Peng, A near-infrared fluorescent probe for selective detection of HClO based on Se-sensitized aggregation of heptamethine cyanine dye, *Chem. Commun.*, 2014, **50**, 1018–1020.
23 F. Lu and T. Nabeshima, A highly selective and sensitive turn-on chemodosimeter for hypochlorous acid based on an iridium(III) complex and its application to bioimaging, *Dalton Trans.*, 2014, **43**, 9529–9536.
24 Y. He, Y. Xu, Y. Shang, S. Zheng, W. Chen and Y. Pang, An ESIPT-based fluorescent probe for the determination of

hypochlorous acid (HClO): mechanism study and its application in cell imaging, *Anal. Bioanal. Chem.*, 2018, **410**, 7007–7017.

25 M. Z. K. Baig, D. Majhi, R. N. P. Tulichala, M. Sarkarb and M. Chakravarty, Easy access to new anthracenyl p-conjugates: generation of distinct AIE-active materials, *J. Mater. Chem. C*, 2017, **5**, 2380–2387.

26 D. Chen, W. Wu, Y. Yuan, Y. Zhou, Z. Wana and P. Huang, Intense multi-state visible absorption and full-color luminescence of nitrogen-doped carbon quantum dots for blue-light-excitable solid-state-lighting, *J. Mater. Chem. C*, 2016, **4**, 9027–9035.

27 X. Zhang, W. Zhao, B. Li, W. Li, C. Zhang, X. Hou, J. Jiang and Y. Dong, Ratiometric fluorescent probes for capturing endogenous hypochlorous acid in the lungs of mice, *Chem. Sci.*, 2018, **9**, 8207.

28 Z. Mao, M. Ye, W. Hu, X. Ye, Y. Wang, H. Zhang, C. Li and Z. Liu, Design of a ratiometric two-photon probe for imaging of hypochlorous acid (HClO) in wounded tissues, *Chem. Sci.*, 2018, **9**, 6035.

29 X. Xie, T. Wu, X. Wang, Y. Li, K. Wang, Z. Zhao, X. Jiao and B. Tang, A two-photon fluorescent probe for ratiometric visualization of hypochlorous acid in live cells and animals based on a selenide oxidation/elimination tandem reaction, *Chem. Commun.*, 2018, **54**, 11965.

30 K. Dou, G. Chen, F. Yu, Z. Sun, G. Li, X. Zhao, L. Chen and J. You, A two-photon ratiometric fluorescent probe for the synergistic detection of the mitochondrial SO_2/HClO crosstalk in cells and *in vivo*, *J. Mater. Chem. B*, 2017, **5**, 8389.

31 L. Zhang, J. Ning, J. Miao, J. Liu and B. Zhao, A new ratiometric fluorescent probe for detecting endogenous HClO in living cells, *New J. Chem.*, 2018, **42**, 2989.

32 Z. Zhang, J. Fan, G. Cheng, S. Ghazali, J. Du and X. Peng, Fluorescence completely separated ratiometric probe for HClO in lysosomes, *Sens. Actuators, B*, 2017, **246**, 293–299.

33 M. Qin, D. Jin, W. Che, Y. Jiang, L. Zhang, D. Zhu and Z. Su, Fluorescence response and detection of Cu^{2+} with 2-(2-hydroxyphenyl)benzimidazole in aqueous medium, *Inorg. Chem. Commun.*, 2017, **75**, 25–28.

34 B. Chen, H. Fu, Y. Lv, X. Li and Y. Han, An oxidative cyclization reaction based fluorescent "Turn-On" probe for highly selective and rapid detection of hypochlorous acid, *Tetrahedron Lett.*, 2018, **59**, 1116–1120.

35 L. Chen, S. Park, D. Wu, H. Kim and J. Yoon, A two-photon ESIPT based fluorescence probe for specific detection of hypochlorite, *Dyes Pigm.*, 2018, **158**, 526–532.